ISOTHERMAL DISSOLUTION OF A SPHERICAL PARTICLE WITH A MOVING BOUNDARY IN A FLOW FIELD

DISOLUCIÓN ISOTERMICA DE UNA PARTÍCULA ESFÉRICA CON UNA FRONTERA MÓVIL EN UN FLUJO DE FLUIDO

E. Vázquez-Nava[1*] and C. J. Lawrence[2]

[1]*Centro de Investigaciones en Ciencia y Tecnología de los Alimentos, Instituto de Ciencias Agropecuarias, Universidad Autónoma del Estado de Hidalgo, Tulancingo, Hgo., México.*

[2]*Department of Chemical Engineering and Chemical Technology, Imperial College London, London SW7 2BY, UK.*

Received 14 April 2007; Accepted 4 July 2007

Abstract

Numerical solution for isothermal dissolution process of a spherical particle with a moving boundary and the presence of hydrodynamics effects of two different flow fields in a binary solution is described in this paper. The flow fields considered are slow viscous flow or Stokes flow and straining motion or shear flow around the particle. The parabolic differential equations were discretised with finite difference method in space, and the resulting set of ordinary differential equations on time was solved by the method of lines. The analysis includes the radial convective term generated due to the density differences between the solid and liquid phases. The effect due to the natural convection caused by density differences between both phases are evaluated and compared with the effect due to the low Reynolds convective flow field. The numerical solution for the isothermal dissolution of a spherical particle in a binary melt is not only compared with integral method for small times of the process but also the results are verified with mass balance integration. The integral method solutions are found to agree with the numerical results for small time of dissolution.

Keywords: dissolution, moving boundary, spherical particle, Stokes flow, shear flow.

Resumen

Una solución numérica para el proceso de disolución isotérmico de una partícula esférica con valores a la frontera móvil con la presencia de efectos hidrodinámicos de dos diferentes flujos de fluido en una solución binaria es descrita en el presente artículo. Los dos flujos a considerar son flujo viscoso lento o flujo de Stokes y flujo de corte o cizalla alrededor de la partícula. Las ecuaciones diferenciales parabólicas fueron discretizadas con el método de diferencias finitas en las coordenadas radial y angular; el sistema de ecuaciones diferenciales ordinarias con respecto al tiempo fue resuelto por el método de líneas. El análisis incluye el termino convectivo radial que se genera debido a la diferencia en densidad entre la fase sólida y líquida. El efecto de la convección natural debido a esta diferencia en densidad entre ambas fases es comparado con el efecto debido a la convección producida debido a flujo con pequeños valores del número de Reynolds presentes en el proceso. Los resultados numéricos de la disolución isotérmica de una partícula esférica en una solución binaria no solo son comparados con el método integral para pequeños tiempos del proceso sino también los resultados son verificados con un balance de integración de masa. Las soluciones por el método integral se encontraron acordes con los resultados numéricos para pequeños tiempos de disolución.

Palabras clave: disolución, frontera móvil, partícula esférica, flujo de Stokes, Flujo de corte o cizalla.

1. Introduction

The change of phase from solid to liquid state and vice-versa is commonly observed in nature, just to mention some, the melting of ice in rivers and lakes, and during volcanic activities, say, cooling lava flows. There are many technical processes in metallurgy, such as casting, welding materials, and crystal growth from melts, in which the control of the solid-liquid phase change is of utmost importance for the quality of the fabricated product.

The rate of dissolution of silica quartz grains in glass making process and pores during sintering from a nearly isolated spherical particle of finite radius is, in many cases, controlled by inter-diffusion, and in some others, controlled by convection. A

* *Autor para la correspondencia*: *E-mail: evazquezn@gmail.com*
Tel (+52-771)-71-72-000 ext 4641, Fax (+52-775)-75-33-495.

Publicado por la Academia Mexicana de Investigación y Docencia en Ingeniería Química A.C.

quantitative model for this process requires derivation and solution of the mass transfer governing equation from the sphere with a moving boundary.

Glass batch melting in industrial scale has been studied under various conditions in order to optimize and control the melting process by many researches (Beerkens *et. al.*, 1994 and Nemec, 1995a, 1995b and 1995c). It has been found that the dissolution phenomena plays an important role on the melting process of the glass batch. The conversion of batch to glass in the industrial process is governed by the rate of dissolution of the particles, and hence, the influence of internal melting factors on the diffusivity has been studied extensively by Cable and Frade, (1987a, 1987b and 1994). The melting of glass is extremely complex, it also involves surface reactions which has been examined by Hrma (1980), (1982), and Bodalbhai and Hrma, (1986).

The dissolution process necessarily occurs with concentration gradients in the liquid phase and convection arises under the action of density differences between both phases. Gelder and Guy (1975) pointed out that this influences not only the rate of dissolution but also the mass solute distribution in the liquid phase of a binary system. Readey and Cooper (1966) solved the dissolution problem in the absence of hydrodynamics effects taking into account the self-induced radial convection generated by the density differences during phase transition. Ruckenstein and Davis (1970) solved the diffusion-controlled growth or collapse of a spherical body that is moving within a surrounding fluid for low Reynolds numbers and potential flow for cases with a small depth of mass diffusion penetration inside the liquid.

When considering an isolated spherical particle in a binary melt, transport properties vary considerably between both phases, which result in totally different rates of mass transport from one phase to another. The fluid density is not a constant but varies locally with the solute composition. Although the fluid can be treated as incompressible, the density variation across the interface needs to be considered.

It is the purpose of this study to establish the differential governing equations for the process of isothermal dissolution of a spherical particle with a moving boundary within a flow field and solve them numerically for several cases of dissolution.

2. Mathematical formulation.

2.1 Governing equations

The partial differential governing equation for describing the process when a pure solid is dissolved in a binary solution is formulated from the conservative equations of momentum and mass:

$$\mu\,\nabla^2 u = 0 \tag{1}$$

$$\frac{\partial C}{\partial t} + u.\nabla C = D\nabla^2 C \tag{2}$$

Since the velocity is not considered to depend on the concentration, the system of equations is solved semi-coupled. Numerical solution is found by obtaining first the velocity profiles from the momentum equation. Two flow fields are considered here, slow uniform viscous flow and straining motion past a sphere. For both cases the radial convective term generated due to the density differences between the solid and liquid phases is included. Due to the linearity in composition with respect to momentum, this convective flow field extra term is simply added to the mass transfer governing equation.

The velocity profile for slow viscous flow, normally found in literature as Stokes Flow (Bird, *et.al.,* 1960), is easily obtained from expression (1):

$$v_r = v_\infty \cos\theta \left[\frac{3}{2}\left(\frac{h}{r}\right) - \frac{1}{2}\left(\frac{h}{r}\right)^3 - 1\right] \tag{3}$$

$$v_\theta = v_\infty \sin\theta \left[1 - \frac{3}{4}\left(\frac{h}{r}\right) - \frac{1}{4}\left(\frac{h}{r}\right)^3\right] \tag{4}$$

On the other side, the velocity profile for straining motion or shear flow (Vázquez-Nava, 2005) around the sphere is written next:

$$v_r = Ah\left(1 - 3\cos^2\theta\right)\left[\left(\frac{h}{r}\right)^2\left(\frac{5}{2} - \frac{3}{2}\left(\frac{h}{r}\right)^2\right) - \left(\frac{r}{h}\right)\right] \tag{5}$$

$$v_\theta = 3\,Ah\,\cos\theta\,\sin\theta\left[\left(\frac{r}{h}\right) - \left(\frac{h}{r}\right)^4\right] \tag{6}$$

where A is a shear rate constant.

The mass transfer governing equation not only has to consider the convective velocity terms due to the flow field but it also has to include the radial fluid motion around the particle due to the differences in volume between liquid and solid phase. According to Readey and Cooper, (1966), the change of density at the liquid-solid system generates a fluid motion in the radial direction:

$$v_r^* = \left(\frac{h}{r}\right)^2 (1 - \vartheta)\frac{dh}{dt} \tag{7}$$

where $\vartheta = \rho_S / \rho_A$.

Therefore, this last convective term is added to the compositional governing expression (2) in order to incorporate the effect due to the density differences between the solid and liquid phases, which describes the dissolution process for any flow field around the spherical solid particle and written next:

$$\frac{\partial C}{\partial t} + v_r\frac{\partial C}{\partial r} + \frac{v_\theta}{r}\frac{\partial C}{\partial \theta} = \frac{D}{r^2}\frac{\partial}{\partial r}\left(r^2\frac{\partial C}{\partial r}\right) + \frac{D}{r^2\sin\theta}\frac{\partial}{\partial\theta}\left(\sin\theta\frac{\partial C}{\partial\theta}\right) + v_r^*\frac{\partial C}{\partial r} \tag{8}$$

$$t = 0 \quad C = C_i \quad r = h(t), \quad C = C_m \quad r > h(t)$$

$$C = C_i \qquad \text{when} \qquad r = h(t), \quad 0 \le \theta \le \pi$$

$$C = C_m \qquad \text{when} \qquad r \to \infty, \quad 0 \le \theta \le \pi$$

The total rate of mass transferred from the spherical particle to the liquid phase according to ideas exposed in Ruckenstein and Davis (1970) is expressed as:

$$\frac{dm}{dt} = \int_0^{\pi} \left(2\ \pi\ h^2 \sin\theta\right) j\big|_{r=h}\ d\theta \tag{9}$$

where the mass flux density of solute is:

$$j = u.C - D\frac{\partial C}{\partial r} \tag{9a}$$

and:

$$u = v_r^* - \frac{dh}{dt} \tag{9b}$$

The convective term velocity in the radial direction at the interface, v_r^*, is the same stated in equation (7). When evaluated at the interface ($r = h(t)$) and according to these last couple of equations, expression (9) becomes:

$$\frac{dm}{dt} = -4\ \pi\ h^2\ C_i\ \frac{\rho_s}{\rho_A}\left(\frac{dh}{dt}\right) - 2\pi\ h^2 D \int_0^{\pi} \left(\frac{\partial C}{\partial r}\right)_{r=h} \sin\theta\ d\theta \tag{10}$$

On the other side, the rate of mass change from the sphere to the liquid is also expressed as:

$$\frac{dm}{dt} = -4\ \pi\ h^2\ \rho_s \frac{dh}{dt} \tag{11}$$

These two last formulae lead to an equation for the moving boundary position at the liquid-solid interface:

$$\frac{dh}{dt} = \frac{D}{2\rho_s\left(1 - C_i/\rho_A\right)} \int_0^{\pi} \left(\frac{\partial C}{\partial r}\right)_{r=h} \sin\theta\ d\theta \tag{12}$$

2.2 Numerical solution

The analysis for the dissolution of a spherical particle in a flow field with a constant thermodynamic equilibrium at the interface due to isothermal conditions is simplified by making the mass balance dimensionless. It is convenient to reduce the equations by carrying out the next substitutions:

$$\hat{C} = \frac{C - C_m}{C_i - C_m}, \qquad \hat{r} = \frac{r}{h_o}, \qquad \hat{t} = \frac{Dt}{h_o^2}, \qquad \hat{h} = \frac{h}{h_0}, \qquad \beta_m = \frac{\left(C_i - C_m\right)}{\rho_s\left(1 - C_i/\rho_A\right)} \tag{13}$$

For this particular case the dimensionless velocity profile and Péclet number definitions are established next for slow viscous flow and straining motion respectively:

$$\hat{v}_r = \frac{v_r}{v_\infty}, \qquad \hat{v}_\theta = \frac{v_\theta}{v_\infty}, \qquad Pe = \frac{v_\infty h_o}{D}$$
$$\hat{v}_r = \frac{v_r}{Ah_o}, \qquad \hat{v}_\theta = \frac{v_\theta}{Ah_o}, \qquad Pe = \frac{Ah_0^2}{D} \tag{14}$$

After transformation, the mass transfer governing equation becomes:

$$\frac{\partial \hat{C}}{\partial \hat{t}} + Pe\left[\hat{v}_r \frac{\partial \hat{C}}{\partial r} + \frac{\hat{v}_\theta}{\hat{r}} \frac{\partial \hat{C}}{\partial \theta}\right] = \frac{1}{\hat{r}^2}\frac{\partial}{\partial \hat{r}}\left(\hat{r}^2 \frac{\partial \hat{C}}{\partial \hat{r}}\right) + \frac{1}{\hat{r}^2 \sin\theta}\frac{\partial}{\partial \theta}\left(\sin\theta \frac{\partial \hat{C}}{\partial \theta}\right) + \hat{v}_r^* \frac{\partial \hat{C}}{\partial \hat{r}} \tag{15}$$

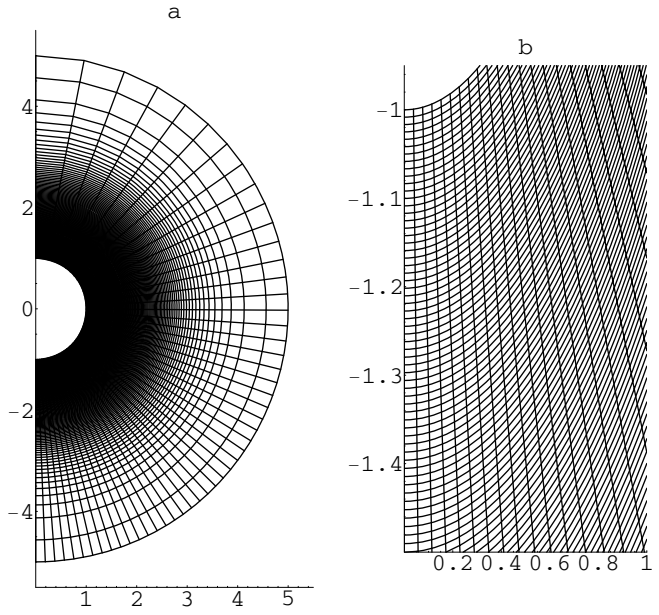

Fig. 1. Grid distribution for particle dissolution in slow uniform viscous flow.

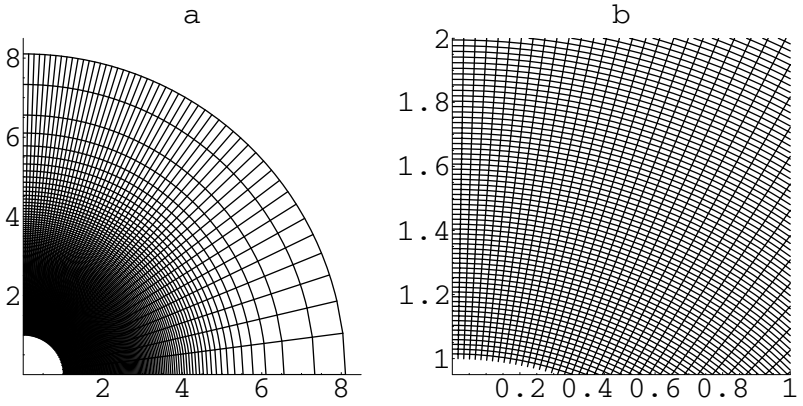

Fig. 2: Grid distribution for particle dissolution in a straining motion.

Then, the integro-differential equation (12), which contains information about the moving boundary position, is written as:

$$\frac{d\hat{h}}{d\hat{t}} = \frac{\beta_m}{2}\int_0^{\pi}\left(\frac{\partial \hat{C}}{\partial \hat{r}}\right)_{\hat{r}=\hat{h}} \sin\theta \, d\theta \qquad (16)$$

It is convenient not only to get the moving boundary fixed by employing a coordinate transformation in the radial direction but also to do a transformation in the angular direction in order to achieve better resolution in the transverse direction for the wake of slow viscous flow, according to the same ideas suggested in literature (Mei and Lawrence, 1996). The governing equations are modified with the next coordinate transformation (ξ,ϕ):

$$\xi = \tanh\left[\gamma_r\left(r-h\right)\right], \qquad 0<\xi<1$$
$$\phi = 1-\frac{\tanh\left[\gamma_\theta\left(1-\theta/\pi\right)\right]}{\tanh\left[\gamma_\theta\right]}, \quad 0<\phi<1 \qquad (17)$$

where γ_r and γ_θ are arbitrary constants, which adjust the grid density along space. Numerical computation is performed using γ_r = 0.3, γ_θ =1.5. The mesh distribution generated with these last couple of equations is shown in Fig. 1. The grid points, which goes from *0* to π, are allocated in order to achieve better resolution near the bottom of the spherical body.

A successful transformation is the one which, whenever possible, improves the convergence of the finite difference solutions. The change of variable modifies the coordinate system *(r,θ)* to another coordinate system *(ξ,ϕ)*. It transforms the map where the composition field is naturally described into a unitary map of coordinates for the dissolution process. For moving boundary problems in particular, it alleviates the difficulties generated in the boundary condition at the interface establishing a fixed domain, instead of having a moving coordinate map.

For straining motion or shear flow around a dissolving particle, the governing equations are written in transformed coordinates *(ξ,ϕ)* according to the next couple of expressions:

$$\xi = \tanh\left[\gamma_r\left(r-h\right)\right], \qquad 0<\xi<1$$
$$\phi = \frac{\tanh\left[\gamma_\theta\left(2\theta/\pi\right)\right]}{\tanh\left[\gamma_\theta\right]}, \quad 0<\phi<1 \qquad (18)$$

where γ_r and γ_θ, are arbitrary constants, which adjust the grid density along space. Numerical computation is performed using γ_r = 0.21, γ_θ =1.75.The mesh distribution generated with these last set of equations, which goes from *0* to $\pi/2$, is shown in Fig. 2. For shear flow, the grid points are allocated in order to achieve a better resolution at the top and bottom of the spherical body. Numerical computations were performed with n_r =150 grid points and n_θ = 50 grid points for both flow fields; with this arrangement, the numerical resolution turns out to be usually sufficient.

Carrying out the transformations the mass governing equation become:

$$\frac{\partial \hat{C}}{\partial \hat{t}} = f_1\frac{\partial^2 \hat{C}}{\partial \xi^2} + f_2\frac{\partial \hat{C}}{\partial \xi} + f_3\frac{\partial^2 \hat{C}}{\partial \phi^2} + f_4\frac{\partial \hat{C}}{\partial \phi} \qquad (19)$$

where f_1, f_2, f_3 and f_4 are functions of the form $f(\xi,\phi)$, naturally generated due to the coordinate transformations, written next:

$$f_1 = f_d, \qquad f_2 = f_a - f_b - f_c + f_f + f_j$$
$$f_3 = f_h, \qquad f_4 = f_g - f_i - f_c$$

where f_a, f_b, f_c… are defined for slow viscous flow (Stokes flow):

$$f_a = \frac{d\hat{h}}{d\hat{t}}\frac{d\xi}{d\hat{r}}, \qquad f_b = \hat{v}_r\frac{d\xi}{d\hat{r}}, \qquad f_c = \frac{\hat{v}_\theta}{\hat{r}}\frac{d\phi}{d\theta},$$
$$f_d = \left(\frac{d\xi}{d\hat{r}}\right)^2, \qquad f_e = 2\xi\gamma_r\frac{d\xi}{d\hat{r}}, \qquad f_f = \frac{2}{\hat{r}}\frac{d\xi}{d\hat{r}},$$
$$f_g = \frac{1}{\hat{r}^2}\frac{d\phi}{d\theta}\cot\theta, \qquad f_h = \frac{1}{\hat{r}^2}\left(\frac{d\phi}{d\theta}\right)^2,$$

$$f_i = \frac{1}{\hat{r}^2}\frac{d\phi}{d\theta}\left[\left(\frac{2\gamma_\theta}{\pi}\right)(\phi-1)\tanh(\gamma_\theta)\right],$$

$$f_j = \left(\frac{\hat{h}}{\hat{r}}\right)^2(\vartheta-1)\frac{d\hat{h}}{d\hat{t}}\frac{d\xi}{d\hat{r}},$$

$$\frac{d\xi}{d\hat{r}} = \gamma_r\left(1-\xi^2\right),$$

$$\frac{d\phi}{d\theta} = \left(\frac{\gamma_\theta}{\pi}\right)\frac{\left[1-\left[(1-\phi)\tanh(\gamma_\theta)\right]^2\right]}{\tanh(\gamma_\theta)}$$

$$\hat{v}_r = \left[\frac{3}{2}\left(\frac{\hat{h}}{\hat{r}}\right)-\frac{1}{2}\left(\frac{\hat{h}}{\hat{r}}\right)^3-1\right]\cos\theta$$

$$\hat{v}_\theta = \left[1-\frac{3}{4}\left(\frac{\hat{h}}{\hat{r}}\right)-\frac{1}{4}\left(\frac{\hat{h}}{\hat{r}}\right)^3\right]\sin\theta$$

Similar expressions were obtained for the straining motion case (Vázquez-Nava, 2005).

At the interface, the moving boundary velocity expression (16), which it has already been properly modified according to the respective coordinate transformation, is integrated by the trapezium rule and become a part of the system of differential equations that has to be solved with those generated from the governing equation (19). Finally, the set of differential equations is solved by the method of lines.

The method of lines technique converts the partial differential equation into a set of simultaneous ordinary differential equations. These equations can be quite stiff (Shastri and Allen, 1998), possibly one of the reasons in the method of lines not being a popular technique. The system of ordinary differential equations depending on time was solved numerically with the aid of DDASSL fortran subroutines, which employ backward differentiation formulas. The subroutine, designed by Linda Petzold, belongs to a collection of mathematical software, papers and databases called netlib, which is also available on the internet (http://www.netlib.org/ode/ddassl.f).

3. Comparison of results

3.1 Integral method

Finite difference methods allow us to carry out simulations for the whole dissolution process. It is the purpose of this section to establish a solution when the mass transfer has just begun and the distance of penetration of mass diffusion from the particle into the liquid phase is short. This small distance of penetration, 'δ', is associated with a boundary layer thickness so that the solution provides not only the depth layer thickness but also automatically establishes the moving boundary location.

There exists no exact solution for the problem of mass transport in a continuous liquid phase from a single spherical particle within a viscous flow field, which is described with the mass transfer governing equation:

$$\frac{\partial C}{\partial t}+v_r\frac{\partial C}{\partial r}+\frac{v_\theta}{r}\frac{\partial C}{\partial \theta} = D\left[\frac{1}{r^2}\frac{\partial}{\partial r}\left(r^2\frac{\partial C}{\partial r}\right)\right]+v_r^*\frac{\partial C}{\partial r} \quad (20)$$

Particularly, this expression does not take into account how composition varies with respect to the angular position for the integral solution, since only a very small thickness of penetration is considered. Boundary conditions for this last equation are:

$$C = C_i \quad \text{when} \quad r = h(t) \quad (21)$$

$$C = C_m \quad \text{when} \quad r \to \infty \quad (22)$$

The equation for the moving boundary remains the same as before for the numerical solution:

$$\frac{dh}{dt} = \frac{D}{2\rho_s\left(1-C_i/\rho_A\right)}\int_0^\pi\left(\frac{\partial C}{\partial r}\right)_{r=h}\sin\theta\, d\theta \quad (23)$$

The continuity equation is written as:

$$\frac{1}{r^2}\frac{\partial}{\partial r}\left(\rho\, r^2 v_r\right)+\frac{1}{r\sin\theta}\frac{\partial}{\partial\theta}\left(\rho\, v_\theta\sin\theta\right)=0 \quad (24)$$

The established penetration distance 'δ' has special properties, such that for $r > \delta$ there is no mass transferred beyond that point. For all practical purposes, at the interface $r = h(t)$, there exist constant thermodynamic equilibrium conditions. In order to simplify the solution, a coordinate transformation is defined as:

$$\hat{z} = \hat{r} - \hat{h} \qquad \hat{r} = \hat{z} + \hat{h} \quad (25)$$

The scaling for the mass governing equation for slow viscous flow is the same as in the numerical solution. Expressions (20) and (24) are added together in order to obtain an expression more easily integrated, which in dimensionless form become:

$$\frac{\partial\hat{C}}{\partial\hat{t}}+\frac{\partial}{\partial\hat{z}}\left(\hat{v}_r\hat{C}\right)+\frac{2}{\hat{h}}\left(\hat{v}_r\hat{C}\right)+\frac{1}{\hat{h}}\frac{\partial}{\partial\theta}\left(\hat{v}_\theta\hat{C}\right)+\cot\theta\frac{\hat{v}_\theta\hat{C}}{\hat{h}} = \frac{2}{\hat{h}}\frac{\partial\hat{C}}{\partial\hat{z}}+\frac{\partial^2\hat{C}}{\partial\hat{z}^2}+\vartheta\frac{d\hat{h}}{d\hat{t}}\frac{\partial\hat{C}}{\partial\hat{z}} \quad (26)$$

If the diffusion boundary layer is thin then it is only the velocity distribution near to the particle surface that is required. The velocity distribution in the region $\hat{z} << \hat{h}$, is obtained by expanding the velocity profile expressions for slow viscous flow in power of $\hat{z}/\hat{h}$, similar expressions can be obtained for straining motion or shear flow (Vázquez-Nava, 2005). For small $\hat{z}/\hat{h}$ it is obtained:

$$\hat{v}_r = 0 \qquad \hat{v}_\theta = \frac{3}{2}\left(\frac{\hat{z}}{\hat{h}}\right)Pe\sin\theta \quad (27)$$

The technique developed here for mass transport is basically the same known in literature as von

Karman-Pohlhausen method for boundary layer theory. The diffusion convective equation is integrated over the boundary layer thickness from *0* to δ, the resulting expression is called the integral equation. The concentration profile will be compelled to satisfy the integral equation but not the original mass transfer governing equation. The mass balance equation will, thereby, be satisfied only in an average sense.

Expression (26) is integrated from *0* to δ to generate the integral equation:

$$\frac{\partial}{\partial \hat{t}}\int_0^{\delta} \hat{C}\, d\hat{z} + \frac{1}{\hat{h}}\frac{\partial}{\partial \theta}\int_0^{\delta}\left(\hat{v}_\theta \hat{C}\right) d\hat{z} + \frac{\cot\theta}{\hat{h}}\int_0^{\delta}\left(\hat{v}_\theta \hat{C}\right) d\hat{z} = -\frac{2}{\hat{h}} - \left(\frac{\partial \hat{C}}{\partial \hat{z}}\right)_{\hat{z}=0} - \vartheta\frac{d\hat{h}}{d\hat{t}} \tag{28}$$

The choice of a satisfactory approximation for the concentration profile is acknowledged to be an important step when employing the integral method approach. For this particular case, the concentration is approximated by a second order polynomial:

$$\hat{C} = \left(1 - \frac{\hat{z}}{\delta}\right)^2 \tag{29}$$

The use of a higher-order polynomial, does not necessarily improve the accuracy of the solution (Caldwell and Chiu, 2000). The polynomial equation has already been arranged to be consistent with the boundary conditions. Integral method results are more accurate when the process have had short time of progress so that the composition profile is well described with a second order expression (29). This polynomial together with the integral equation (28) generates the next differential equation for slow viscous flow:

$$\frac{4}{3}\frac{d\delta}{dt} + Pe\sin\theta\left(\frac{\delta}{\hat{h}}\right)\frac{d}{d\theta}\left(\frac{\delta}{\hat{h}}\right) + Pe\cos\theta\left(\frac{\delta}{\hat{h}}\right)^2 = 8\left(\frac{1}{\delta} - \frac{1}{\hat{h}}\right) - 4\vartheta\frac{d\hat{h}}{d\hat{t}} \tag{30}$$

where:

$$\frac{d\hat{h}}{d\hat{t}} = \frac{\beta_m}{2}\int_0^{\pi}\left(\frac{\partial \hat{C}}{\partial \hat{z}}\right)_{\hat{z}=0}\sin\theta\, d\theta = -\beta_m\int_0^{\pi}\frac{\sin\theta}{\delta}d\theta \tag{31}$$

The last couple of differential equations gives the integral method solution. The obtained results, although not exact, are often sufficiently accurate for engineering purposes.

3.2 Mass balance integration

Analytical methods offer an exact solution, but due to the nonlinear nature of the moving boundary, the mass governing equation that describes the dissolution of a spherical particle has to be solved numerically. When a numerical technique is employed there always exists an uncertainty about accuracy in the results.

Integral method is restricted in the range of validity for small period of time so that the results were not expected to be valid for the whole dissolution process. For this reason, mass balance integration was implemented in order to be able to verify the obtained answer from the numerical solution.

The mass transfer governing equation is written in its dimensionless form:

$$\frac{\partial \hat{C}}{\partial \hat{t}} + \hat{v}_r\frac{\partial \hat{C}}{\partial r} + \frac{\hat{v}_\theta}{\hat{r}}\frac{\partial \hat{C}}{\partial \theta} = \frac{1}{\hat{r}^2}\frac{\partial}{\partial \hat{r}}\left(\hat{r}^2\frac{\partial \hat{C}}{\partial \hat{r}}\right) + \frac{1}{\hat{r}^2\sin\theta}\frac{\partial}{\partial \theta}\left(\sin\theta\frac{\partial \hat{C}}{\partial \theta}\right) + \hat{v}_r^*\frac{\partial \hat{C}}{\partial \hat{r}} \tag{32}$$

This equation can be integrated between the limits from '*0*' to 'π' in the angular direction and from '*h(t)*' to '∞' in the radial direction together with the velocity expressions for slow viscous flow and the next following expression is obtained:

$$2\pi\frac{\partial}{\partial \hat{t}}\int_0^{\pi}\int_{\hat{h}}^{\infty}\hat{C}\,\hat{r}^2\sin\theta\, dr d\theta = -\left(\frac{1}{\beta_m} + \vartheta\right)\frac{d}{d\hat{t}}\left(\frac{4\,\pi\,\hat{h}^3}{3}\right) \tag{33}$$

The last equation allows to verify numerical results, simulations turn out to deviate by less than 0.1 % from the expected value when comparing numerical results from both sides of the equation, which gives confidence in the obtained results for describing the isothermal dissolution within a low Reynolds flow field.

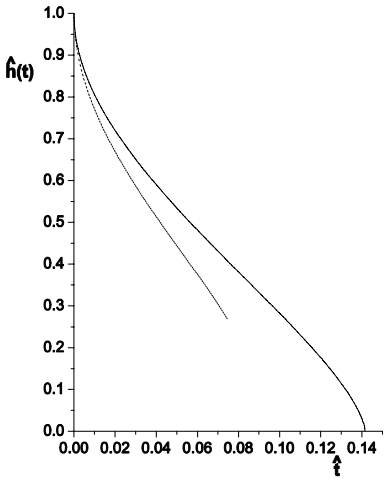

Fig. 3: Rate of dissolution in uniform slow viscous flow $t_{end} \approx 0.14$. The dashed line represents the integral method solution and the solid line represents the numerical solution (Pe = 5.0, β_m = 3.0, ϑ = 0.5).

4. Results and discussion

Integral method predicts quite the same as numerical solution does when isothermal dissolution within a flow field has just evolved a small period of time, as illustrated in Fig. 3. Finite differences solution generates a set of differential equations to be solved for each grid point, numerical computations were performed with 150 x 50 nodes. Integral method requires only 253 differential equations to be solved.

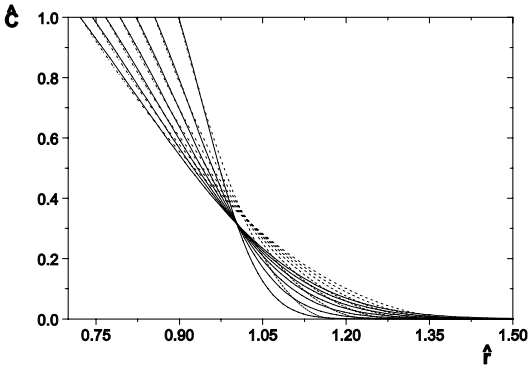

Fig. 4: Composition profile evolution at $\theta = \pi$ when $\hat{t} \approx 0.018$ (Pe = 5.0, β_m = 3.0, ϑ = 0.5, t_{end} = 0.14).

At the particle bottom, integral method was expected not to describe properly the process because mass diffusion thickness increases sharply at this point due to slow viscous flow direction, in spite of this adverse circumstance, there were acceptable results for short periods of time, as shown in Fig. 4. However, not for all physical conditions was possible to obtain same flatter results. Fig. 5 illustrates conditions where not only the slow viscous flow field is diminished but also the mass gradient driving force around the particle is weaker. Particularly, for such conditions, integral method was expected to give a much better prediction, however the density change parameter, affect also markedly the dissolution process. It is clearly evident

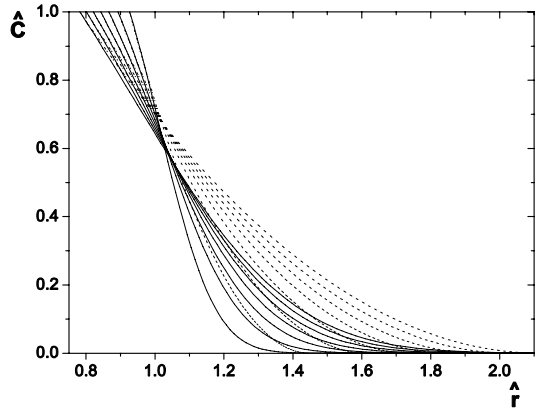

Fig. 5: Composition profile evolution at $\theta = \pi$ when $\hat{t} \approx 0.05$ (Pe = 2.5, β_m = 1.5, ϑ = 1.5, t_{end} = 0.39).

that the number of competing effects involved in the process are so many that the complex nature of the event cannot be satisfactorily described by employing an expression (20) where composition diffuses just a small thickness of penetration.

There always exists an uncertainty about results when a solution is obtained through numerical techniques. Integral method was implemented in order to verify, somehow, that both solutions predict approximately similar results within the range of validity of integral method. Mass balance integration become a more reliable method in order to verify numerical results, simulations turn out to deviate by less than 0.1% from the expected value, which gives confidence for the numerical results as an acceptable description for the isothermal dissolution within a low Reynolds flow field.

Two types of advective terms are competing during isothermal dissolution: the radial convective fluid motion due to the density differences between both phases and the convective terms included due to the low Reynolds flow field around the particle. When the density change parameter takes $\vartheta < 1.0$ values, the rate of dissolution increases rather than it does for values of $\vartheta > 1.0$, as shown in Fig. 6, this is explained because for $\vartheta < 1.0$ values there exist a decrease in volume during phase transition, which generates a fluid motion toward the interface; the opposite situation occurs for values of $\vartheta > 1.0$. This liquid motion may be interpreted as suction and/or blowing effect across the interface. Same figure also illustrates how the rate of sphere shrinkage increases while slow viscous flow field takes higher Péclet values. It is worth to mention that these conditions were the best obtained results in order to show a significant increase on the rate of dissolution. The process is not strongly affected by slow viscous flow around the sphere, similar results were also obtained for shear flow either.

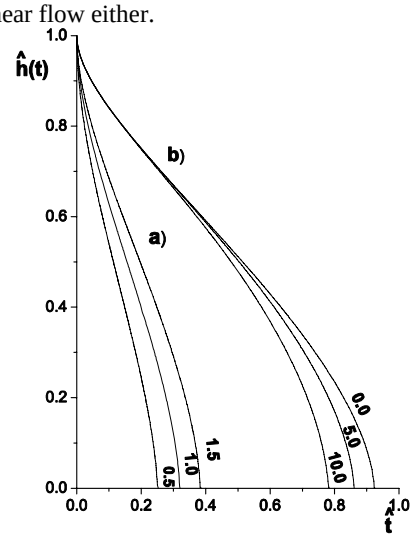

Fig. 6: Rate of dissolution in uniform slow viscous flow, a) Pe = 5.0 and β_m = 1.5 for ϑ = 0.5, 1.0,1.5 b) β_m = 0.5 and ϑ = 1.5 for Pe = 0.0, 5.0, 10.0.

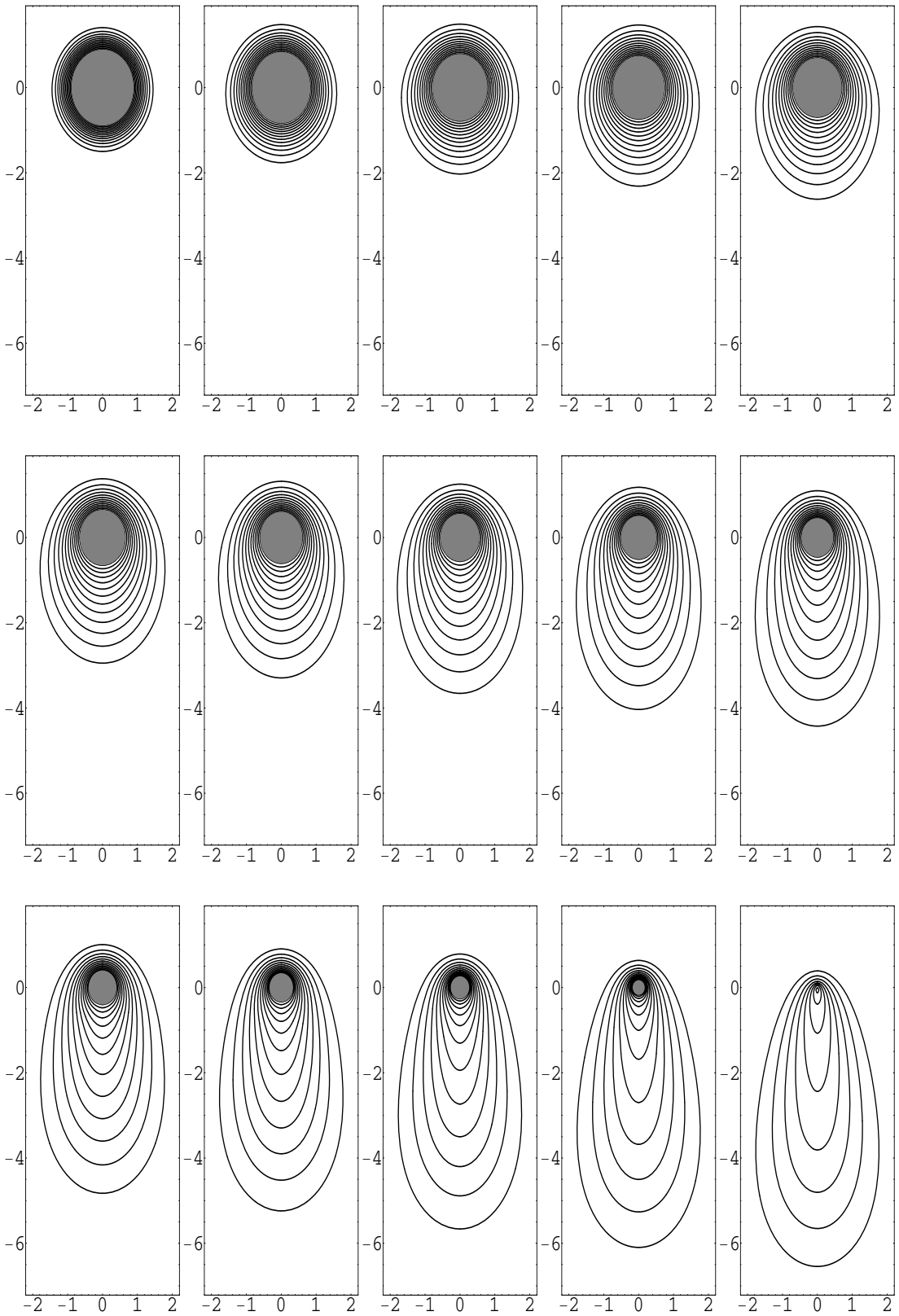

Fig. 7: Isotherm contours around a dissolving particle within uniform slow viscous flow, the process occurs in 15 stages equally distributed on time ($t_{end} \approx 0.78$, $Pe = 10.0$, $\vartheta = 1.5$, and $\beta_m = 0.5$).

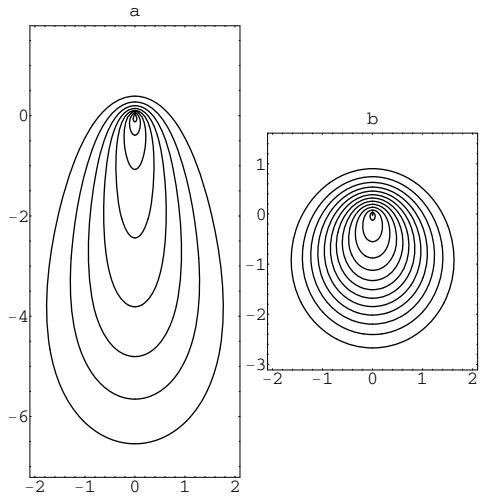

Fig. 8: Isotherm contours at the end of particle dissolution in uniform slow viscous flow, a) $t_{end} \approx 0.78$ (Pe = 10.0, ϑ = 1.5, β_m = 0.5), b) $t_{end} \approx 0.19$ (Pe = 10.0, ϑ = 1.5, β_m = 5.0).

Stokes or slow viscous flow affects sensibly the mass solute distribution around the stationary particle in a binary liquid melt, as illustrated in Fig. 7. The rate of dissolution around the sphere is influenced very weakly when Péclet number varies. At the particle top, mass hardly diffuses due to the flow field direction and boundary layer is very thin; since fluid is incompressible, thickness may seems to move according to the interface position. Compositional differences between the solid and the melt significantly affect the rate of sphere shrinkage, as illustrated in Fig. 8. Mass driving force, which is taken into account in the parameter β_m , influences not only the dissolution time but also the mass solute distribution around the particle, while density change parameter ϑ and convection due to the flow field included in the Péclet number are maintained constant.

Similar results were obtained for the isothermal dissolution within straining motion or shear flow around the sphere, as illustrated in Fig. 9. Contribution of convective transport due to the flow field intensity expressed in the Péclet number do not affect the dissolution time but it does influence the mass solute distribution around the particle, as shown in Fig. 9 a) and 9 b). With Pe and ϑ constant, increases in β_m parameter decreases the time it takes for the process to finished and also mass diffusion around the particle become clearly affected as seen by comparing Fig.s 9 a) and 9 c). The mass driving force influence the rate of dissolution more pronounced than it does the convective transport from the flow field.

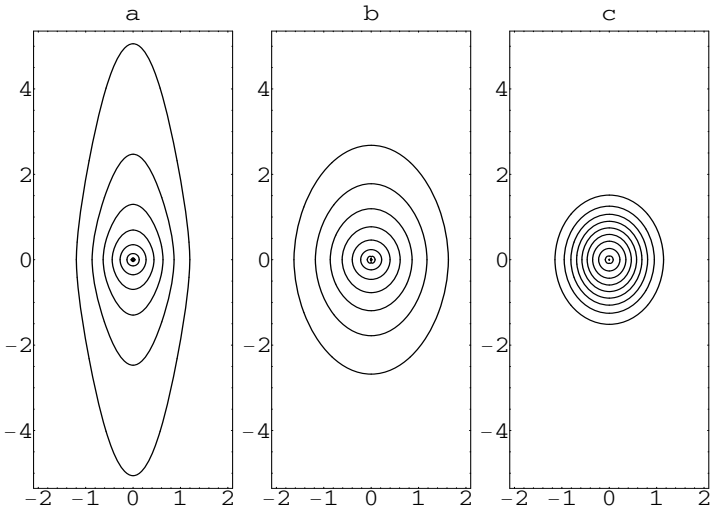

Fig. 9: Isotherm contours around the particle at the end of dissolution during straining motion a) $t_{end} \approx 0.72$ (Pe = 1.5, ϑ = 0.5, β_m = 0.5), b) $t_{end} \approx 0.74$ (Pe = 0.5, ϑ = 0.5, β_m = 0.5), c) $t_{end} \approx 0.1$ (Pe = 1.5, ϑ = 0.5, β_m = 5.0).

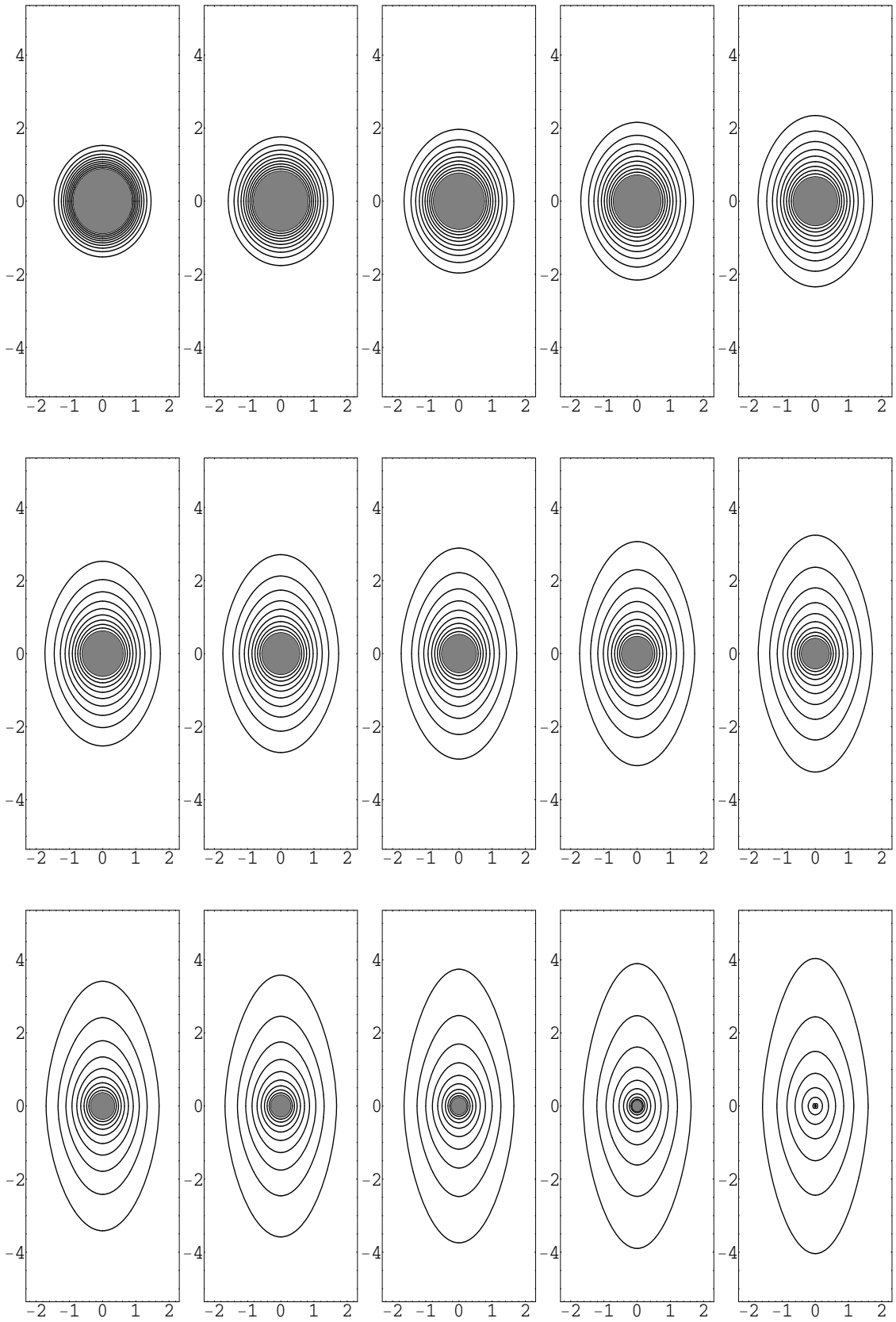

Fig. 10: Isotherm contours around a dissolving particle within straining motion, the process occurs in 15 stages equally distributed on time ($t_{end} \approx 0.91$, Pe = 0.75, ϑ = 1.5, and β_m = 0.5).

The obtained results, in terms of the rate of sphere shrinkage, are similar for both straining motion and slow viscous flow. Flow field mostly increases notoriously the dissolution rate during the last stages of the process, when the available surface area for mass diffusion becomes smaller in comparison to the original particle. At this very end of the process, the rate of dissolution tend to increase markedly in the presence of the flow field, this effect dominate, no matter the increased solute concentration around the tiny particle. Isotherm patterns with Péclet number equal to 0.75 for the full progress of dissolution phenomena within straining motion are shown in Fig. 10. Mass solute distribution around the spherical particle is increased naturally at the top and bottom of the particle due to the flow field.

Concluding remarks

At the very beginning of the process, when the evolved time is small enough for composition profile to be described with a second order approximation (29), integral and numerical solution were found to be in closed agreement for many obtained results. However, not for all physical conditions was possible to obtain an acceptable approximation. Mass balance integration did offer a more effective route in order to verify numerical results.

The density change parameter during isothermal dissolution, which naturally arises as a convective term, generates a fluid motion toward the interface if the liquid is more dense and away from the interface if the solid is denser as a result of mass conservation. This radial fluid motion due to density differences during phase transition in some circumstances may influence more pronouncedly than it does the slow convective flow field.

The time taken for finishing the process decreases when compositional difference between the solid and the melt increases. Mass driving force influences the rate of dissolution more pronouncedly than it does the convective transport from the flow field. Convective transport mostly distributes the solute around the sphere according to the fluid flow direction. Dissolution time is not accelerated significantly due to the flow because the liquid motion has low Reynolds number. At the last stages, not only the smaller available particle surface for mass transport influenced the rate of dissolution but clearly also the flow field shows more effectively its effects in spite of the increased amount of solute around the tiny sphere.

Acknowledgments

This work received support by Consejo Nacional de Ciencia y Tecnologia in Mexico. E. Vázquez-Nava wishes to acknowledge his debt of gratitude to Vidriera Queretaro for the valuable experience obtained through the years he worked for them. We would like to thank to Professor Richard V. Craster for much helpful guidance and for the many constructive suggestions.

Nomenclature

Roman Letters

A	shear rate constant
C	mass concentration
D	binary diffusion coefficient
f	numerical functions from coordinate transformation.
h	interface position as a function of time
j	mass flux density of solute
m	mass
Pe	Péclet number
r	radial coordinate
t	time
u	velocity
v	velocity due to flow field
v_r^*	radial fluid motion due to the change of density
z	coordinate transformation for integral method

Greek Symbols

μ	viscosity
θ	angular coordinate
ρ	mass density
ϑ	density change parameter
β	dimensionless parameter
ξ	radial coordinate transformation
ϕ	angular coordinate transformation
γ	stretching coordinate parameter
δ	boundary layer thickness

Subscripts

A	refers to the pure solute in liquid state
end	refers to the end of the process
i	refers to the equilibrium interface
m	refers to the far field liquid melt
o	refers to initial conditions
s	refers to the solid
r	refers to radial direction
θ	refers to angular direction
∞	refers to far field position

Superscripts

^	refers to a dimensionless variable

References

Beerkens, R.G.C., Muijsenberg, H.P.H.,Van der Heijden, T. (1994). Modelling of sand grain dissolution in industrial glass melting tanks. *Glasstech. Ber. Glass Science Technology 67* (7), 179-188.

Bird, R.B., Stewart, W.E., Lighfoot, E. (1960). Transport Phenomena. *John Wiley & Sons, Inc.,* New York.

Bodalbhai, L., Hrma, P. (1986). The dissolution of silica grains in isothermally heated batches of

sodium carbonate and silica sand. *Glass Technology 27* (2), 72-78.

Caldwell, J., Chiu, C.K. (2000). Numerical solution of one-phase Stefan problems by the heat balance integral method, Part I – Cylindrical and spherical geometries. *Communications in Numerical Methods in Engineering 16*, 569-583.

Cable, M., Frade, J.R. (1987a). The diffusion-controlled dissolution of spheres. *Journal of Material Science 22*, 1894-1900.

Cable, M., Frade, J.R. (1987b). Diffusion-controlled mass transfer to or from spheres with concentration-dependent diffusivity. *Chemical Engineering Science 42*(11), 2525-2530.

Cable, M., Frade, J.R. (1994). Diffusion-controlled growth or dissolution of spheres with variable temperature. *Journal of the American Ceramic Society 77* (4), 999-1004.

Gelder, D., Guy, A.G. (1975). Current problems in the glass industry. In Ockendon and Hodgkins (1975), pp 71-90.

Hrma, P. (1980) A kinetic equation for interaction between grain material and liquid with application to glass melting. *Silikaty 24*, 7-16.

Hrma, P. (1982) Thermodynamics of batch melting. *Glasstech. Ber. Glass Science Technology 55*, (7), 138-150.

Mei, R., Lawrence, C.J. (1996). The flow fiel due to a body in impulsive motion. *Journal of Fluid Mechanics 325*, 79-111.

Nemec, L. (1995a). Energy consumption in the glass melting process. Part 1: Theoretical relations. *Glasstech. Ber. Glass Science Technology 68*(1), 1-10.

Nemec, L. (1995b). Energy consumption in the glass melting process. Part 2: Results of calculations. *Glassteck.Ber. Glass Science Technology 68*, (2), 39-49.

Nemec, L. (1995c). Some critical points of the glassmelting process: Part 1: Dissolution phenomena. *Ceramics-Silikaty 39* (3), 81-86.

Ockendon, J.T., Hodkins, W.R. (1975) *Moving boundary problems in heat flow and diffusion.* Clarendon Press, Oxford.

Readey, D.W., Cooper, Jr. A.R. (1966). Molecular diffusion with a moving boundary and spherical symmetry. *Chemical Engineering Science 21*, 917-922

Ruckenstein, E., Davis, E.J. (1970). Diffusion-controlled growth or collapse of moving and stationary fluid spheres. *Journal of Colloid and Interface Science 34* (1), 142-158.

Shastri, S.S., Allen, R.M. (1998). Method of lines and enthalpy method for solving moving boundary problems. *International Communications of Heat and Mass Transfer 25*(4), 531-540.

Vázquez-Nava, E. (2005). *Thermal and Isothermal Dissolution of a Spherical Particle*. PhD Thesis. Imperial College London.